Liquid Crystals
Publication details, including instructions for authors and subscription information:
http://www.informaworld.com/smpp/title~content=t713926090

Helix unwinding process in the chiral smectic C phase of MHPOBC as observed by conoscopy

Shun-Ichi Suwa[a]; Yoichi Takanishi[a]; Hajime Hoshi[a]; Ken Ishikawa[a]; Hideo Takezoe[a]
[a] Department of Organic and Polymeric Materials, Tokyo Institute of Technology, O-okayama, Meguro-ku, Tokyo 152-8552, Japan,

Online publication date: 11 November 2010

To cite this Article Suwa, Shun-Ichi , Takanishi, Yoichi , Hoshi, Hajime , Ishikawa, Ken and Takezoe, Hideo(2003) 'Helix unwinding process in the chiral smectic C phase of MHPOBC as observed by conoscopy', Liquid Crystals, 30: 4, 499 — 505
To link to this Article: DOI: 10.1080/0267829031000091147
URL: http://dx.doi.org/10.1080/0267829031000091147

LIQUID CRYSTALS, 2003, VOL. 30, NO. 4, 499–505

Helix unwinding process in the chiral smectic C phase of MHPOBC as observed by conoscopy

SHUN-ICHI SUWA, YOICHI TAKANISHI, HAJIME HOSHI, KEN ISHIKAWA and HIDEO TAKEZOE*

Department of Organic and Polymeric Materials, Tokyo Institute of Technology, O-okayama, Meguro-ku, Tokyo 152-8552, Japan

(*Received 6 December 2002; accepted 27 December 2002*)

Conoscopic studies have been made on the helix unwinding process in the chiral smectic C phase of MHPOBC. The unwinding process is rather unique in the sense that abrupt changes of the biaxiality and apparent tilt angle are followed by further gradual changes before the complete helix unwinding. The process is qualitatively explained by simulating the conoscopic images using the 4×4 matrix method with consideration of model molecular distributions, by taking account of both the ferroelectric and dielectric coupling between molecules and a field. The transmittance loss due to selective reflection was also measured under the application of a stepwise d.c. field. The shift of the dip position due to the loss, toward a longer wavelength region, was observed at low field. In contrast, the emergence of a transmittance loss at the same wavelength as that of an unperturbed state was observed. This phenomenon is explained by the ferroelectric deformation of a helix with the pitch unchanged.

1. Introduction

The chiral smectic C (SmC*) liquid crystal phase has a smectic layer structure where molecules are tilted with respect to the layer normal. Because of the chiral molecules, the symmetry of the system is reduced to C_2, with the C_2 symmetry axis parallel to the layer and perpendicular to the molecular long axis. Hence, an in-layer polarization may appear along the C_2 axis. Also because of the chirality, the tilted molecules form a helical structure with the helical axis along the layer normal. Thus, a ferroelectric liquid crystal phase is realized, although overall polarization is cancelled due to the helical structure, i.e. helielectric structure.

This helical structure is easily removed by applying an electric field parallel to the layer, due to the coupling between in-layer polarization and the electric field. The helix unwinding process has previously been studied both experimentally [1–3] and theoretically [3–7]. Here we report a detailed investigation of the helix unwinding process in the SmC* phase of 4-(1-methylheptyloxycarbonyl)phenyl 4′-octyloxybiphenyl-4-carboxylate (MHPOBC).

Conoscopy is a very powerful method for investigating the biaxial structure. It has been successfully used to identify phase structures such as the antiferroelectric and ferrielectric phases [8, 9]. Besides the identification of phase structures, this technique is useful for investigating the helix unwinding process, since the tilt of optic axes and biaxiality can be analysed. Conoscopy indicates how the average optic axis tilts and how biaxiality arises under the application of an electric field.

The electric field-induced evolution of conoscopic figures in MHPOBC was reported by Gorecka *et al.* [8]. The threshold electric field for the complete unwinding of helix was defined as the field strength where abrupt change occurs from a uniaxial structure to a biaxial one. However, the induced tilt of the optic axis is much smaller than the tilt angle determined by other methods. Thus, the previous conoscopic measurements did not reach the critical part of the helix unwinding process. This motivates the present measurements. To achieve our purpose, conventional transmittance measurements were also adopted, giving characteristic dips due to selective reflection.

2. Experimental procedure

The sample used was *S*-MHPOBC, whose chemical structure and phase sequence are shown in figure 1. The material was introduced into sandwich cells with substrates treated homeotropically using silane coupling agent (Toray Dow-Corning, AY43-21) or polyimide surface alignment layer (Nissan Chemical, RN1211). The cell thickness was about 300 μm.

The set-up for conoscope observation used was a standard system, except for the use of a He-Cd laser

*Author for correspondence;
e-mail: htakezoe@o.cc.titech.ac.jp

Liquid Crystals ISSN 0267-8292 print/ISSN 1366-5855 online © 2003 Taylor & Francis Ltd
http://www.tandf.co.uk/journals
DOI: 10.1080/0267829031000091147

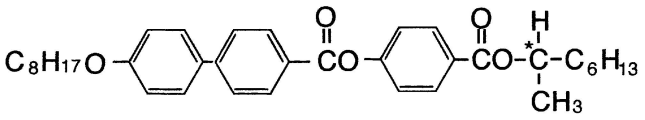

SmA-(120.2°C)-SmCα*-(118.7°C)-SmC*
-(117.2°C)-SmCγ*-(116.3°C)-SmCA*

Figure 1. Chemical structure and phase sequence of MHPOBC.

(442 nm, IK5651R-G, Kinmon) as light source [8, 10, 11]. The use of a short wavelength has the advantage of obtaining a large phase difference between two optical polarizations, producing more rings in the figure. An objective lens (×40, WD 10 mm, NA 0.5) was used for the incident converging beam. The sample was held in a temperature-controlled oven to regulate the temperature with accuracy better than 0.01°C. An electric field was applied parallel to the substrate with electrodes separated by 1 mm. The conoscopic images obtained under the application of an electric field were recorded by a digital video camera, and sent to a computer for data analysis by a standard method [8].

Transmittance spectra were measured using a microscope spectrometer (400–800 nm, TFM-120AFT, ORC) under the application of an electric field. The measurement at a longer wavelength region was made using a conventional spectrometer (Hitachi U-3400).

3. Results

3.1. *Conoscopy*

Figure 2 shows a series of conoscopic figures taken at 0.4°C below the SmA–SmC* phase transition. In the absence of a field, a uniaxial conoscopic figure is observed because of the uniform helix winding. On application of a small field such as 10 V mm^{-1}, a slight shift of the figure toward the direction perpendicular to the field is observed, although the appearance of biaxiality is hardly visible. At 16.25 V mm^{-1}, abrupt changes occur both in the biaxiality and apparent tilt angle. Further change occurs between 137.5 and 150 V mm^{-1}, after a gradual change between 16.25 and 137.5 V mm^{-1}.

These changes are quantitatively shown in figure 3, where biaxiality, $n_y - n_x$, and apparent tilt angle are shown. In a low field regime below about 16 V mm^{-1}, the apparent tilt angle gradually increases to 3°. In this regime, the biaxiality scarcely changes. At 16.25 V mm^{-1}, an abrupt change occurs in both the apparent tilt angle and the biaxiality. Gorecka *et al.* [8] attributed this change to the complete helix unwinding. However, the tilt angle of about 10° is much smaller than the 17° measured by a conventional microscopic observation using a homogeneously aligned cell. With further increase of the electric field, the apparent tilt angle increases to 14°, and finally a rather abrupt increase to 17° is observed around 140–160 V mm^{-1}. In contrast, the biaxiality gradually decreases after the sharp increase at 16.25 V mm^{-1} and shows a rather abrupt decrease at about 150 V mm^{-1}. After these abrupt changes at about 150 V mm^{-1}, both the apparent tilt angle and the biaxiality stay almost constant.

3.2. *Selective reflection*

Transmittance spectra also give information of the helix unwinding process. Figure 4 shows the transmittance spectra observed at various field strengths. In the absence of a field, a very clear dip (transmittance loss of about 50%) is observed and is attributed to the selective reflection. On the application of a field, the transmittance dip shifts to a longer wavelength and becomes broader. This indicates that the helical pitch has lengthened and the helical structure become distorted, resulting in a wide distribution of helical pitch. Another interesting feature of the spectra is the emergence of an additional peak at the original helical pitch wavelength above 70 V mm^{-1}.

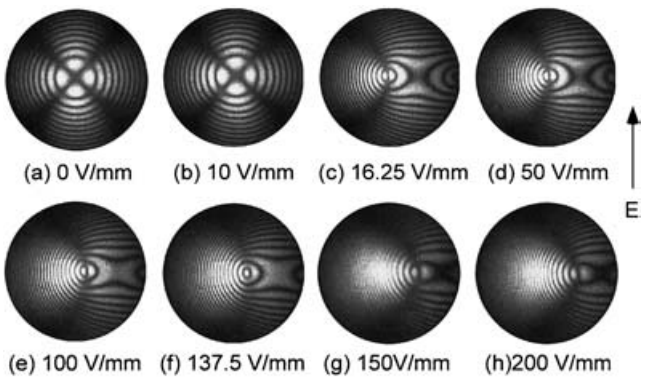

Figure 2. Conoscopic images under the application of stepwise d.c. fields of various strengths.

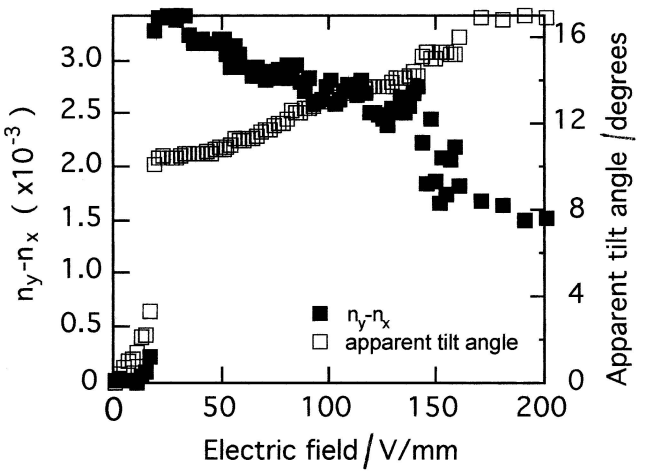

Figure 3. Biaxiality and apparent tilt angle as a function of applied electric field.

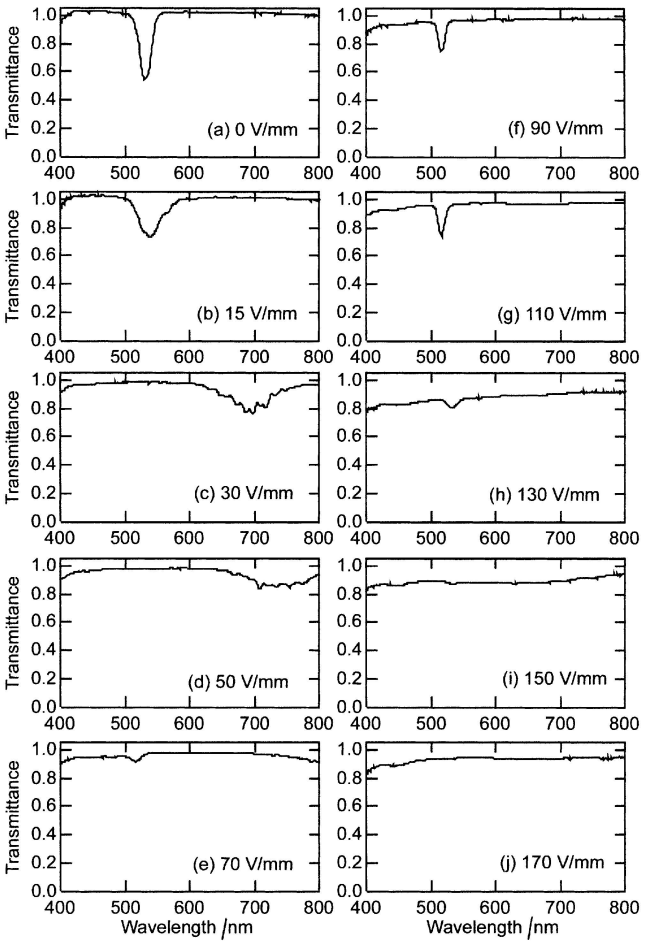

Figure 4. Transmittance spectra under various electric field strengths.

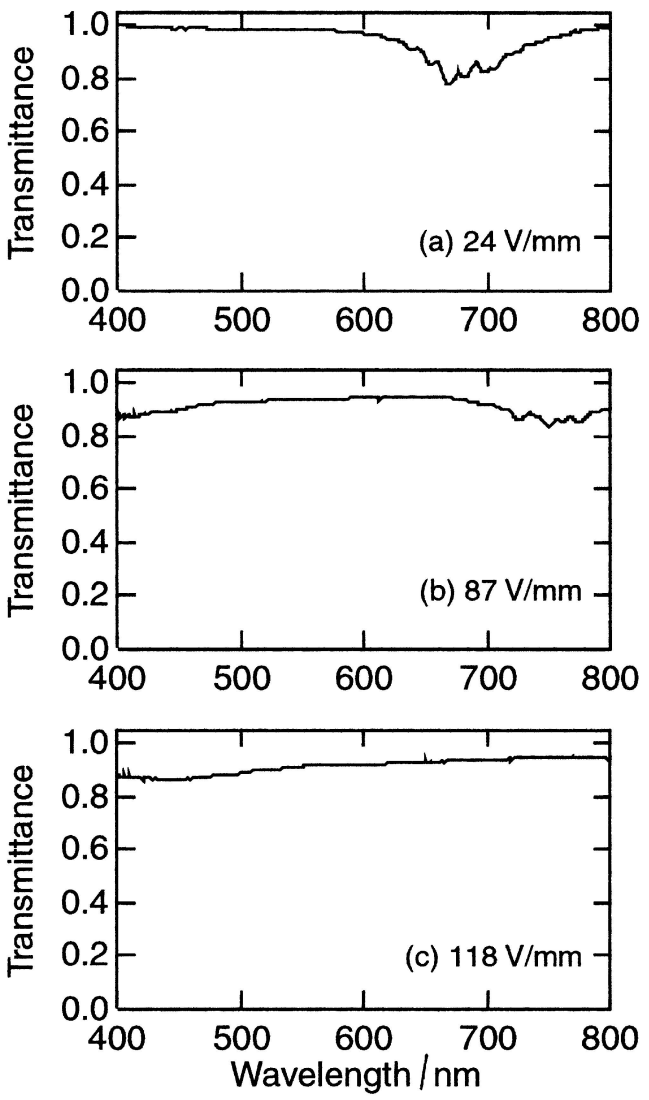

Figure 5. Transmittance spectra (*a*) after the application of a stepwise field of 24 V mm^{-1}, and (*b*) after gradually increasing the field from 24 to 87 V mm^{-1} and (*c*) to 118 V mm^{-1}.

This peak shows a slight blue shift at 130 V mm^{-1}, and finally disappears at about 150 V mm^{-1}, at which complete helix unwinding occurs. It is worth noting that a broad peak (not shown) is also observed at the wavelength corresponding to about twice the pitch. This peak is attributed to a full pitch band [12, 13] and is observed because of the asymmetric deformation of the helix. So, why is the asymmetrically deformed helix, with the same pitch as that in the absence of a field, stabilized at a higher field?

In order to clarify this problem, selective reflection measurements were carried out under the two-step field application. Thus, a stepwise d.c. field of 24 V mm was applied first, and was then gradually increased to 118 V mm^{-1}. The results are shown in figure 5. At 24 V mm^{-1}, a red-shifted broad reflection loss is observed as in figure 4 (*c*). On increasing the field to 87 V mm^{-1}, this reflection loss shifts further to longer wavelength and is less pronounced. No structure remains at 118 V mm^{-1}. Note that there is a dip corresponding to the selective reflection of an unperturbed helix, when a stepwise field is applied in the range 87–118 V mm^{-1}, as shown in figures 4 (*e–g*).

The key to understanding the difference lies in the different field application processes. Because of the instantaneous high field application in figure 4, helix deformation with the pitch unchanged occurs, so that the transmittance loss appears at the wavelength corresponding to the unperturbed helical pitch. In contrast, once a small electric field is applied as in the first process in figure 5, the coupling between the electric field and spontaneous polarization distorts the helix, so that the subsequent gradual field application does not produce the same helical condition as in figure 4.

In this way, the deformed helical structures of figure 4 are unstable. This situation is more clearly seen by the change with time of the transmittance spectra. Figure 6 shows the changes with time after applying stepwise d.c. fields. At 15 V mm^{-1}, the original dip remains at the same wavelength with less intensity immediately after applying a field. We can see a gradual change of the dip at 3 and 10 s after field application. At 50 V mm^{-1}, a shifted dip emerges in the beginning and no essential change occurs. At higher field strengths (110 and 150 V mm^{-1}), a small peak is observed at the original dip position. The dip finally disappears in both cases, though it remains longer under 150 V mm^{-1}. This is consistent with the mechanism mentioned above, since an instantaneous application of a higher field stabilizes the 2π wall (2π-soliton), as will be discussed in the next section. The gradual change of the helix deformation after applying an electric field was also pointed out by Conradi *et al.* [3].

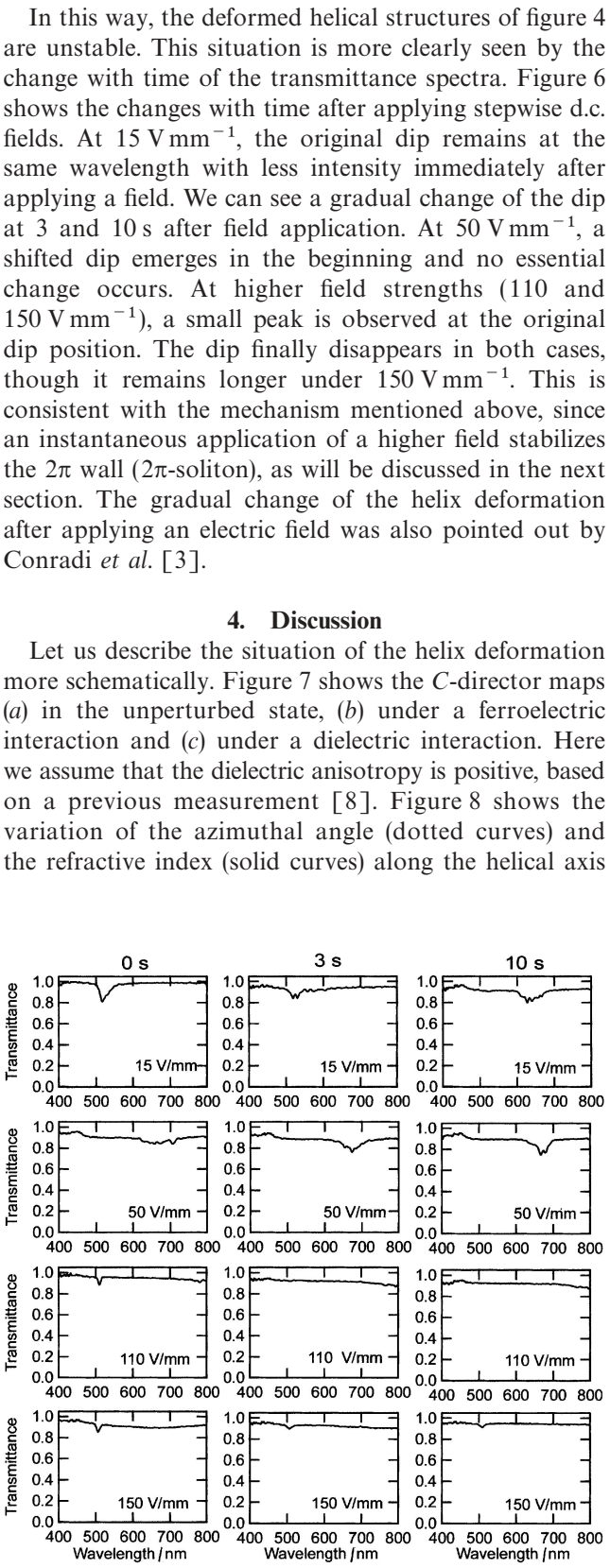

Figure 6. Change of the transmittance spectra with time on application of stepwise fields of various strengths.

4. Discussion

Let us describe the situation of the helix deformation more schematically. Figure 7 shows the *C*-director maps (*a*) in the unperturbed state, (*b*) under a ferroelectric interaction and (*c*) under a dielectric interaction. Here we assume that the dielectric anisotropy is positive, based on a previous measurement [8]. Figure 8 shows the variation of the azimuthal angle (dotted curves) and the refractive index (solid curves) along the helical axis

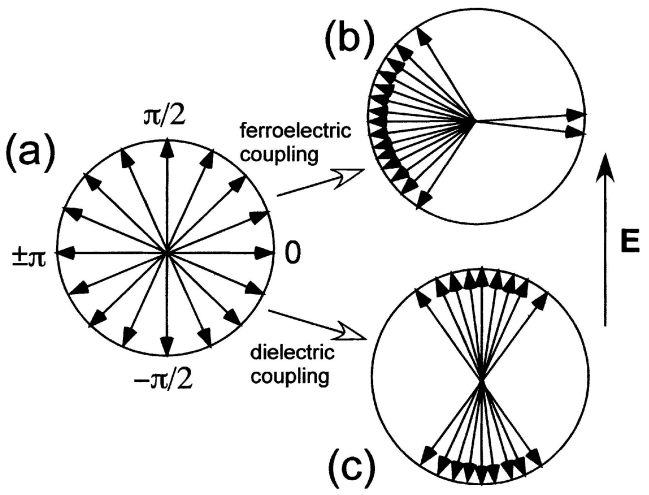

Figure 7. *C*-director orientations in (*a*) unperturbed state, (*b*) under a ferroelectric interaction and (*c*) under a dielectric interaction.

(*a*) in the unperturbed state, (*b*) under a ferroelectric interaction and (*c*) under a dielectric interaction. The ferroelectric coupling between the field and the spontaneous polarization stabilizes the *C*-director orientation at $\Phi = \pi$, with metastable orientation at $\Phi = 0$ remaining, figure 7 (*b*); i.e. a 2π-soliton (2π wall) remains in each period, as shown in figure 8 (*b*). In contrast, the dielectric coupling stabilizes the structure shown in figure 7 (*c*) with two π-solitons (π wall) remaining in each period, as shown in figure 8 (*c*).

The refractive index variation is shown by solid curves in figure 8. The refractive index in the unperturbed state has a periodicity of half the pitch for light propagation along the helical axis. This causes only one reflection, i.e. a selective reflection band, at the wavelength corresponding to one optical pitch, i.e. a structural pitch multiplied by an average refractive index, since the refractive index variation is sinusoidal. Under a dielectric interaction, the period is still a half-pitch, see figure 8 (*c*). Since the structure is no more than sinusoidal, however, higher harmonics corresponding to 1/4, 1/6, 1/8 pitch, etc., may emerge in addition to the fundamental corresponding to 1/2 pitch. The ferroelectric interaction yields a special feature. The periodicity of the refractive index is now a full pitch and is far from a sinusoidal change, as shown in figure 8 (*b*). Hence, one may observe a reflection at the wavelength corresponding to twice an optical pitch (full pitch band). In addition, the higher harmonics of a full pitch, i.e. 1/2, 1/3, 1/4 pitch, etc., could be seen. If the suggested change shown in figure 8 (*b*) occurs without changing the pitch, the transmittance spectra shown in figures 4 (*e–h*) would be obtained. The observation of the full pitch band confirms the existence of the ferroelectric interaction.

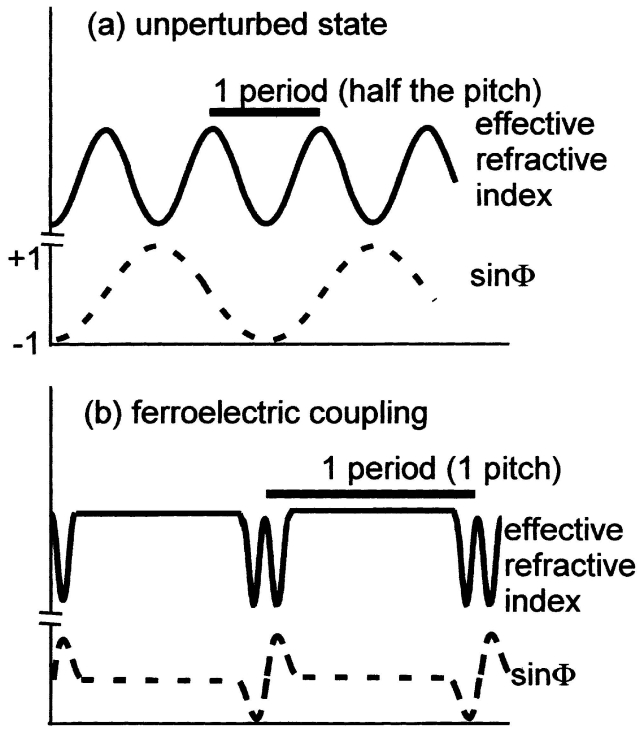

Figure 8. Schematic illustration of the azimuthal angle distribution and the refractive index along the helical axis, (*a*) in the unperturbed state, (*b*) under a ferroelectric interaction and (*c*) under a dielectric interaction.

Now let us consider the conoscopic figures. In a previous paper [11], we showed that the biaxiality $n_y - n_x$ becomes negative under an intermediate electric field before complete helix unwinding in a short pitch SmC* mixture, and that the negative biaxiality is well explained in the framework of the elastic theory and the 4×4 matrix method. Here, x and y are perpendicular and parallel to the field. However, MHOPBC never shows negative biaxiality. How can we explain this?

Figure 9 (*a*) shows a schematic drawing of the azimuthal angle calculated by the elastic theory with only the ferroelectric interaction [14]. This behaviour can be simplified

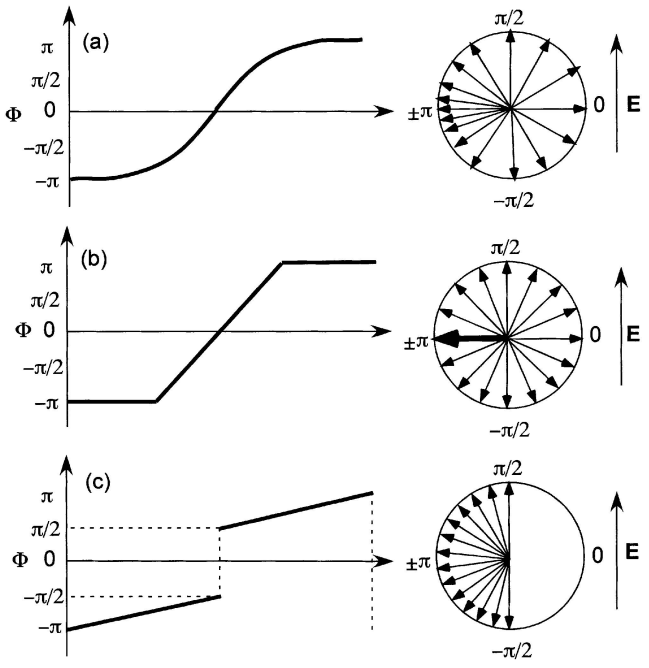

Figure 9. Schematic drawing of the azimuthal angle distribution, (*a*) calculated by the elastic theory with only the ferroelectric interaction, (*b*) a simplified model of (*a*), and (*c*) a special model with a π-soliton.

as in figure 9 (*b*), where a thick arrow stands for a high distribution. The structure is essentially the same as figure 8 (*b*); one period is divided into three parts, i.e. two unwound and one uniform helix regions. We simulated conoscopic images based on this simplified model with a variety of the fraction of helix region. The parameters were chosen according to the materials constants of MHPOBC: $n_1 = 1.5$, $n_2 = 1.501$ and $n_3 = 1.668$; helical pitch = 600 nm, layer spacing = 4 nm and cell thickness = 240 μm. Here n_1 is a refractive index perpendicular to the molecular long axis and the spontaneous polarization direction, n_2—parallel to the spontaneous polarization, and n_3—parallel to the molecular long axis. One pitch consists of 150 layers. We take $2n$ layers for the helix region; $n = 0$ stands for a completely unwound state and $n = 75$ is an unperturbed state.

The simulated conoscopic figures for $n = 75$, 60, 45, 30, 15 and 0 are shown in figure 10. Negative and positive anisotropies are characterized by the splitting of the isogyre along the directions parallel and perpendicular to the field, respectively. Figure 10 reveals that the system shows first negative biaxiality which changes to positive on increasing the field strength. The biaxiality is plotted against n in figure 11. It is found that the biaxiality is negative in most states except for the nearly completely helix unwound region. Thus, the naïve model for helix unwinding does not explain the experimental results.

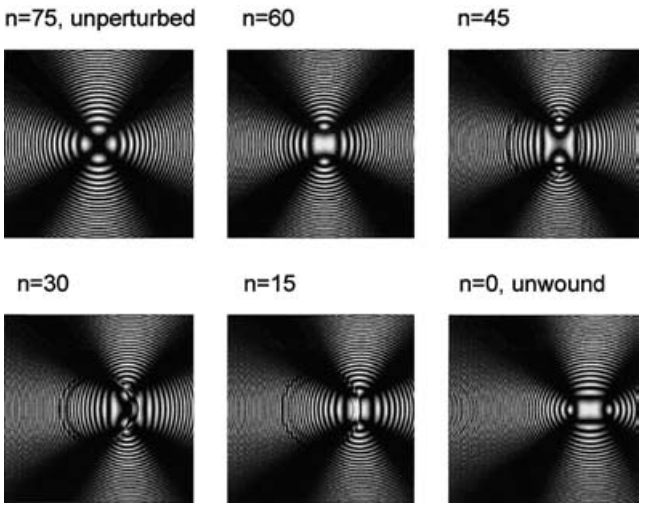

Figure 10. Simulated conoscopic figures calculated by applying the 4×4 matrix method to the simplified model shown in figure 9 (*b*).

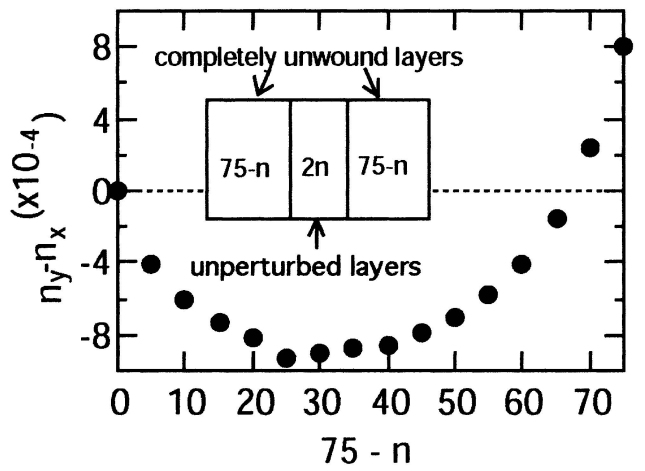

Figure 11. Biaxiality as a function of n for the model shown in figure 9 (*b*).

Let us discuss qualitatively the conditions that give positive biaxiality with a finite average tilt. We start from the simplest molecular arrangement consisting of three molecules in a unit cell. The structure is equivalent to the SmC^*_γ (Sm_{ferri1}) phase represented by the deformed Ising [15] (deformed clock [16]) model shown in figure 12, where the *C*-directors of three molecules in a unit cell are illustrated. When the *C*-directors of the A and B molecules are parallel to each other and antiparallel to that of the C molecule, i.e., $\Psi = 0$ (Ising model), the largest negative biaxiality is obtained and the average tilt is to the right. With increasing Ψ, the biaxiality and the average tilt angle approach zero and attains zero at $\Psi = 60^\circ$ (clock model). In order to explain the experimental results, i.e. positive biaxiality and tilt to the left,

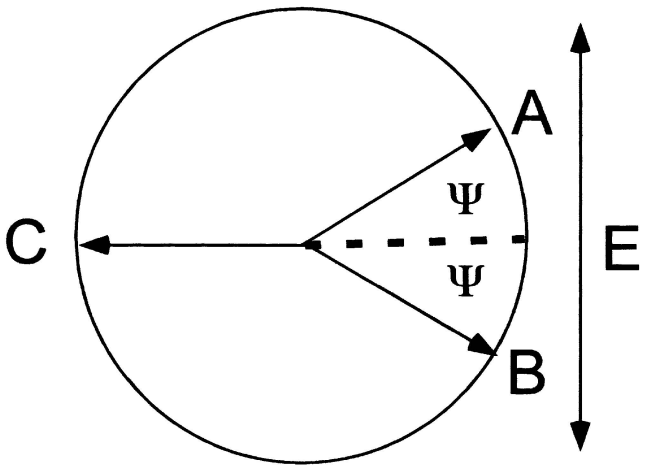

Figure 12. Azimuthal angle distribution in the deformed Ising (clock) model of the SmC^*_γ phase.

Ψ must be larger than 60°. This means that molecules must exist, whose *C*-director is close to the field direction in order to have positive biaxiality.

Based on the foregoing qualitative discussion above, we examined a simplified model structure shown in figure 9 (*c*). This type of molecular distribution could be realized under contributions of both the ferroelectric and dielectric couplings between molecules and a field, as schematically shown in figure 7. The simulated conoscopic image is shown in figure 13, clearly showing positive biaxiality. The obtained biaxiality is 2.4×10^{-3} and the apparent tilt angle is 10.5° when using the same parameters as used for figure 10. These values are in good accordance with the values of those shown between 20 and 150 V/mm, i.e. after an abrupt change and before complete helix unwinding, in the experiment shown in figure 3. If the molecular distribution shown in figure 9 (*c*)

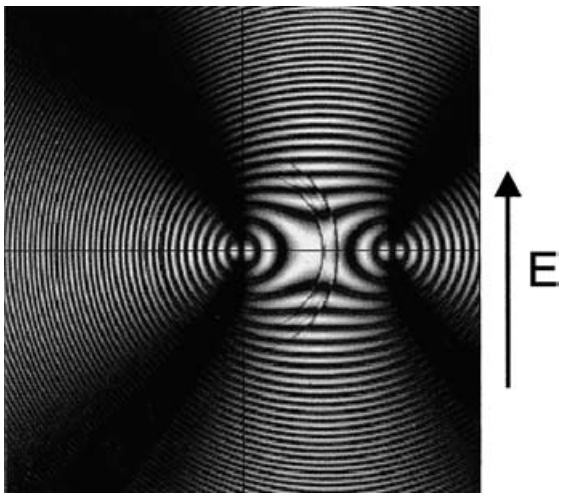

Figure 13. Simulated conoscopic figure for the model molecular distribution described in figure 9 (*c*).

shrinks toward the orientation perpendicular to the field, the biaxiality decreases and the tilt angle increases, being consistent with experiment. This distribution change is possible under the ferroelectric coupling between molecules and a field. However, the cause of the molecular orientation shown in figure 9 (*c*) is not clear at the present stage, and remains a problem for the future.

5. Conclusion

A detailed observation of the conoscopic images in the SmC* phase of MHPOBC has been made. We found a characteristic field dependence of the biaxiality and the apparent tilt angle; specifically, both quantities suddenly increase at low field below 20 $V\,mm^{-1}$ and gradually change until complete helix unwinding at 150 $V\,mm^{-1}$. This behaviour is quite different from that observed in a short pitch ferroelectric liquid crystal mixture. Because of this unique behaviour, a conventional theoretical consideration fails to explain the whole process. We have qualitatively shown that the observed conoscopic images can be explained by taking account of both the ferroelectric and the dielectric coupling between molecules and a field. The transmittance loss due to selective reflection also yields a unique feature, namely the emergence of the transmittance loss at the same wavelength as that in an unperturbed state. This phenomenon is explained by the ferroelectric deformation of a helix with the pitch unchanged. Full theoretical consideration is necessary for the future.

We thank Prof. B. Zeks for helpful discussion. This work is partly supported by a Grant-in-Aid for Scientific Research (#115550003) and on Priority Area (B) (12129202) by the Ministry of Education, Science, Sports and Culture, Japan.

References

[1] Bahr, Ch., Heppke, G., and Sharma, N. K., 1987, *Ferroelectrics*, **76,** 151.
[2] Pavel, J., Glogarova, M., and Bawa, S. S., 1987, *Ferroelectrics*, **76,** 221.
[3] Conradi, M., Kityk, A. V., Skarabot, M., Blinc, R., and Musevic, I., 1999, *Liq. Cryst*., **26,** 1179.
[4] Hudak, O., 1983, *J. Phys. (Fr.)*, **44,** 57.
[5] Dmitrienko, V. E., and Belyakov, V. A., 1980, *Zh. eksp.tior.Fiz*., **78,** 4.
[6] Urbanc, B., Zeks, B., and Carlsson, T., 1991, *Ferroelectrics*, **113,** 207.
[7] Cladisi, P. E., Brand, H. R., and Finn, P. L., 1983, *Phys. Rev. A*, **28,** 512.
[8] Gorecka, E., Chandani, A. D. L., Ouchi, Y., Takezoe, H., and Fukuda, A., 1990, *Jpn. J. appl. Phys*., **29,** 131.
[9] Isozaki, T., Fujikawa, T., Takezoe, H., and Fukuda, A., 1993, *Phys. Rev. B*, **48,** 13439.
[10] Fujikawa, T., Hiraoka, K., Isozaki, T., Kajikawa, K., Takezoe, H., and Fukuda, A., 1993, *Jpn. J. appl. Phys*., **32,** 985.
[11] Suwa, S., Hoshi, H., Takanishi, Y., Ishikawa, K., Takezoe, H., and Zeks, B., *Jpn. J. appl. Phys.* (to be published).
[12] Hori, K., 1983, *Mol. Cryst. liq. Cryst*., **100,** 75.
[13] Ouchi, Y., Shingu, T., Takezoe, H., Fukuda, A., Kuze, E., Koga, M., and Gpto, N., 1984, *Jpn. J. appl. Phys*., **23,** L660.
[14] Urbanc, B., Zeks, B., and Carlsson, T., 1991, *Ferroelectrics*, **76,** 207.
[15] Akizuki, T., Miyachi, K., Takanishi, Y., Ishikawa, I., Takezoe, H., and Fukuda, A., 1999, *Jpn. J. appl. Phys*., **38,** 4832.
[16] Johnson, P. M., Olson, D. A., Pankratz, S., Nguyen, T., Goodby, J., Hird, M., and Huang, C. C., 2000, *Phys. Rev. Lett*., **84,** 4870.